Innovare
Academic Sciences

International Journal of Pharmacy and Pharmaceutical Sciences

ISSN- 0975-1491 Vol 7, Issue 2, 2015

Original Article

TOXICITY AND MOLECULAR DOCKING STUDIES OF TETRAHYDROQUINOLINES AGAINST MICROBIAL, CANCER, RETINOIC ACID RECEPTOR, INFLAMMATORY, CHOLESTEROL ESTER TRANSFERASES AND PARASITIC PROTEIN RECEPTORS

PRADEEP P. SETHUMADHAVAN NAIR[a], KIRAN KUMAR H. CHANDRASHEKARAPPA[a], JAGADEESH N. MASAGALLI[a], PRASHANTHA NAGARAJA[b], KITTAPPA M. MAHADEVAN*[a]

[a]Department of Post Graduate Studies and Research in Chemistry, School of Chemical Sciences, Kuvempu University, P. G. Centre, Kadur, Karnataka 577548, India, [b]Department of Medicinal Chemistry, Scientific Bio-Minds, Bangalore 560092, Karnataka, India.
Email: mahadevan.kmm@gmail.com

Received: 01 Dec 2014 Revised and Accepted: 20 Dec 2014

ABSTRACT

Objective: Synthesis of 2-methoxy-4-(3-methyl-2-phenyl-1,2,3,4-tetrahydroquinolin-4-yl)phenol derivatives (**4a-i**) and to study their inhibitory effects towards inflammatory, cancer, retinoic acid, cholesterol esterase, parasitic and microbial proteins.

Methods: Various 2-methoxy-4-(3-methyl-2-phenyl-1,2,3,4-tetrahydroquinolin-4-yl)Phenols (**4a-i**) were synthesized via imino Diels-Alder reaction and were characterized by IR, ^{1}H NMR, ^{13}C NMR mass spectroscopy and elemental analysis. All 2-methoxy-4-(3-methyl-2-phenyl-1,2,3,4-tetrahydroquinolin-4-yl)Phenols (**4a-i**) and six FDA approved reference drugs were docked against inflammatory, cancer, retinoic acid, cholesterol esterase, parasitic and microbial protein receptors. The results were studied and validated based on molecular docking analysis.

Results: The compounds 4a-i were less toxic on internal tissues and show no side effect. The compounds 4c and 4f were strongly interacts with active site amino acids Arg210, His107, Ala197, Thr198 and Arg195 of binding energy -16.0728 kcal/mol and -56.5169 kcal/mol with inflammatory protein. The compound 4b and 4f binds with cancer protein shows -8.99845 and -5.70191 kcal/mol of energy exhibits significant anticancer properties. The compound 4a shows 7 hydrogen bonds with retinoic acid protein within amino acids Asn1185 and Arg1309 with energy of -47.423 kcal/mol than remaining compounds. The compound 4g shows 5 hydrogen bonds of energy -32.9844 kcal/mol with amino acids Arg155, Gln124, Leu122 with microbial protein. The compounds 4c, 4d and 4i exhibits 3 hydrogen bonds within active site amino acids of energy -8.29829 kcal/mol, against cholesterol esterase protein. Nevertheless, all 4a-i compounds shows strong interaction with parasitic protein.

Conclusion: The compounds 4a, 4c, 4f, 4g, and 4h were identified as multifunctional lead compounds hence; these compounds could be considered as potential lead molecules in the future study.

Keywords: Isoeugenol, Tetrahydroquinoline, Antimicrobial, Anticancer, Anti-inflammatory, Antiparasitic, Antiretinoic acid, Cholesterol esterase, Molecular docking.

INTRODUCTION

Isoeugenol is a natural flavoring agent occurs in various plants includes cloves, dill seeds, nutmeg and sandalwood [1]. Plants produce a monomeric group of phenylpropenes like chavicol, t-anol, eugenol, and isoeugenol is incorporated to inhibit microbial growth [2] and impart medicinal property. Free phenol functional group responsible for effective ranges of antimicrobial and anticancer properties [3]. It was reported that a combined action of Isoeugenol and tetrahydroquinoline derivates exhibited many biological properties include anticancer activity [4]. For example 4-hydroxy-3-methoxyphenyl substituted 3-methyl-tetrahydroquinolines were tested in human tumor cells MCF-7, SKBR-3, PC3, HeLa shows cytotoxic activity in early and later stages [5] and also exhibited antimalarial activity with malarial protein farnesyltransferase (PFT) [6]. The another property of tetrahydroquinoline derivates that shows effective interaction with RARβ, γ retinoic acid receptors exhibit tumor promoter induced ODC (ornithine decarboxylase) activity in hairless mouse skin and posses potential antiretinoic property [7].

Further, the tetrahydroquinoline containing sulphonamide moiety exhibited cytotoxic activity [8, 9] and potent, CRTH2 antagonists properties [10]. Cis-1-benzoyl-2-methyl-4-(phenylamino)-1,2,3,4-tetrahydroquinolines were found to be promising leads for use as inducers in systems to control gene expression based on AaEcR (Aedes aegypti Ecdysone receptor) [11], hence these properties reveals that the tetrahydroquinoline derivates possess diverge biological functions for the treatment of various disease. There were few synthetic methods which include Hetero-Diels–Alder reaction to obtain tetrahydroquinoline moieties [12-16].

Further interesting moiety 4-(p-methoxyphenyl)-3,4-tetra hydroquinolin-2(1*H*)-ones were found to occur in many natural products and reported to exhibit important biological properties (fig. 1), [17-21] i. e., Penigequinolones (1) isolated from the mycelial mats of Penicillium sp., No. 410 were reported as pollen-growth inhibitors [10].

But, the biological properties of tetrahydroquinolines coupled with isoeugenol moiety have still not been explored extensively. Keeping in view of natural occurrence of isoeugenol derivates coupled to tetra hydro qunolines and in continuation of our work on biological activity of heterocyclic compounds [22-30], herein, we report the study of a three-component condensation and cyclo addition reaction between anilines, benzaldehydes and trans-isoeugenol to furnish a new class of 2-methoxy-4-(3-methyl-2-phenyl-1,2,3,4-tetrahydroquinolin-4-yl)phenol derivatives (**4a-i**). To make this hetero Diels-Alder synthetic method more efficient, eco friendly high and yield we succeeded to use acetic acid, in which acetic acid served as both catalyst and solvent. This method is based on our earlier reports in generating novel tetrahydroquinolines for different biological trials [31-35]. All synthesized 2-methoxy-4-(3-methyl-2-phenyl-1,2,3,4-tetra hydroquinolin-4-yl) Phenols (**4a-i**) were subjected to molecular docking studies for antimicrobial, anticancer, retinoic acid receptor, anti-inflammatory, cholesterol ester transferases and antiparasitic activities.

MATERIALS AND METHODS

Chemistry

All chemicals were purchased from commercial sources and were used without further purifications. All the melting points were

recorded in open capillaries and are uncorrected. Silica gel (60-120 mesh) was used for column chromatography and TLC analysis was performed on commercial plates coated with silica gel 60 F_{254}. Visualization of the spots on TLC plates was achieved by UV irradiation.

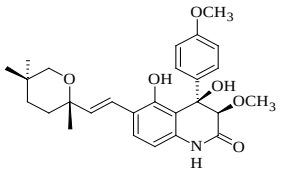

Fig. 1: Naturally occurring 4-(p-methoxyphenyl)-3, 4-tetrahydroquinolin-2(1*H*)-one

Elemental analysis was recorded on vario MICRO CHNS. Mass spectra were recorded on Finnigan Mat 1020 C spectrometer using ionization energy of 70 eV. ^{1}H and ^{13}C NMR spectral analysis were performed on a spectrometer operating at 300 MHz, 400 MHz, and 75 MHz, 100 MHz, respectively in $CDCl_3$ solutions unless otherwise stated. Chemical shifts are reported with respect to tetra methyl silane (TMS) for ^{1}H NMR and the central line (77.0 ppm) of $CDCl_3$ for ^{13}C NMR. Coupling constants (*J*) are reported in Hz. Standard abbreviations s, d, t and m refer to singlet, doublet, triplet and multiplet respectively.

A typical procedure for the synthesis of 4-(6-chloro-3-methyl-2-phenyl-1,2,3,4-tetrahydroquinolin-4-yl)-2-methoxyphenol (4b)

A mixture of p-chloro aniline (0.5 g, 3.91 mmol) and benzaldehyde (0.41g, 3.91 mmol) in acetic acid (20 mL) was stirred at room temperature (25 °C) for 20 min. Finally, *trans*-isoeugenol (0.48 g, 2.93 mmol) was added and the reaction mixture was refluxed for 8-9 h. After the completion of reaction (as indicated by TLC), the reaction mixture was poured into water (50 mL) and extracted with ethyl acetate (3 x 30 mL). The ethyl acetate extract was washed with water, brine solution, dried over anhydrous Na_2SO_4 and concentrated under vacuum. The crude material was purified by column chromatography on silica gel (petroleum ether/ethyl acetate, 9:1 v/v) to give 4-(6-chloro-3-methyl-2-phenyl-1,2,3,4-tetrahydroquinolin-4-yl)-2-methoxyphenol (**4b**) (Yield = 1.0 g, 68 %). Similarly other 2-methoxy-4-(3-methyl-2-phenyl-1,2,3,4-tetrahydroquinolin-4-yl)phenols (**4a-i**) were synthesized.

Spectral data

2-methoxy-4-(7-methyl-6-phenyl-5,6,7,8-tetrahydro-[1,3]dioxolo[4,5-*g*]quinolin-8-yl) phenol (4a)

White amorphous solid; m. p. 220-221 °C; ^{1}H NMR (400 MHz, $CDCl_3$): δ = 8.76 (s, 1 H), 7.45-7.43 (m, 2 H), 7.39-7.35 (m, 2 H), 7.32-7.28 (m, 1 H), 6.73-6.69 (m, 2 H), 6.60-6.58 (m, 1 H), 6.27 (s, 1 H), 5.86 (s, 1 H), 5.74 (d, *J* = 8.0 Hz, 2 H), 5.68 (s, 1 H), 3.98 (d, *J* = 9.6 Hz, 1 H), 3.72 (s, 3 H), 3.57 (d, *J* = 10.8 Hz, 1 H), 2.07-1.99 (m, 1 H), 0.43 (d, *J* = 6.4 Hz, 3 H) ppm; ^{13}C NMR (100 MHz, $CDCl_3$): δ = 147.53, 146.09, 145.49, 144.89, 143.07, 142.87, 140.68, 138.06, 135.62, 128.20, 127.42, 126.82, 121.44, 116.51, 115.33, 114.98, 112.70, 99.69, 95.43, 62.95, 55.63, 54.10, 51.21, 48.21, 16.22 ppm; MS: *m/z* = 390.2 (M+1). Anal. Calcd for $C_{24}H_{23}NO_4$: C, 74.02, H, 5.95, N, 3.60. Found: C, 74.23, H, 6.18, N, 3.79.

4-(6-chloro-3-methyl-2-phenyl-1,2,3,4-tetrahydroquinolin-4-yl)-2-methoxyphenol (4b)

White amorphous solid; m. p. 155-156 °C; ^{1}H NMR (400 MHz, $CDCl_3$): δ = 7.44-7.42 (m, 2 H), 7.40-7.36 (m, 2 H), 7.35-7.33 (m, 1 H), 6.93 (dd, *J* = 2.4, 8.6 Hz, 1 H), 6.89 (d, *J* = 8.0 Hz, 1 H), 6.73 (dd, *J* = 1.6, 8.0 Hz, 1 H), 6.64 (d, *J* = 2.0 Hz, 1 H), 6.57 (s, 1 H), 6.45 (d, *J* = 8.8 Hz, 1 H), 5.58 (s, 1 H), 4.10 (d, *J* = 10.0 Hz, 1 H), 3.85 (s, 3 H), 3.66 (d, *J* = 10.8 Hz, 1 H), 2.18-2.15 (m, 1 H), 0.57 (d, *J* = 6.4 Hz, 3 H) ppm; ^{13}C NMR (75 MHz, $CDCl_3$): δ = 147.28, 144.86, 135.75, 130.04, 129.10, 128.55, 128.32, 127.34, 123.16, 114.65, 111.39, 64.36, 56.45, 52.51, 41.54, 16.87 ppm; MS: *m/z* = 380.1 (M+1). Anal. Calcd for $C_{23}H_{22}ClNO_2$: C, 72.72, H, 5.84, N, 3.69. Found: C, 72.99, H, 6.12, N, 3.95.

4-(6-(3-chlorophenyl)-7-methyl-5,6,7,8-tetrahydro-[1,3]dioxolo[4,5-*g*]quinolin-8-yl)-2-methoxyphenol (4c)

White amorphous solid; m. p. 194-195 °C; ^{1}H NMR (400 MHz, $CDCl_3$): δ = 8.81 (s, 1 H), 7.48-7.42 (m, 4 H), 6.74-6.68 (m, 3 H), 6.61-6.55 (m, 2 H), 6.10-6.07 (m, 1 H), 5.96 (s, 1 H), 4.05 (d, *J* = 9.6 Hz, 1 H), 3.71 (s, 3 H), 3.65 (d, *J* = 11.2 Hz, 1 H), 2.10-2.03 (m, 1 H), 0.44 (d, *J* = 6.8 Hz, 3 H) ppm; ^{13}C NMR (100 MHz, $CDCl_3$): δ = 147.26, 146.78, 144.78, 136.72, 134.93, 130.25, 128.65, 128.42, 126.81, 123.08, 114.37, 111.29, 110.19, 100.95, 64.36, 56.49, 52.67, 42.27, 16.87 ppm; MS: *m/z* = 424.3 (M+1). Anal. Calcd for $C_{24}H_{22}ClNO_4$: C, 68.00, H, 5.23, N, 3.30. Found: C, 68.28, H, 5.64, N, 3.55.

4-(2-(4-chlorophenyl)-6-fluoro-3-methyl-1,2,3,4-tetrahydroquinolin-4-yl)-2-methoxy phenol (4d)

Pale yellow amorphous solid; m. p. 190-191 °C; ^{1}H NMR (400 MHz, $CDCl_3$): δ = 7.27-7.24 (m, 3 H), 6.85 (d, *J* = 8.0 Hz, 1 H), 6.71 (dd, *J* = 2.0, 8.0 Hz, 1 H), 6.62 (d, *J* = 1.6 Hz, 1 H), 6.12-6.10 (m, 2 H), 5.77 (dd, *J* = 1.6, 9.2 Hz, 2 H), 5.50 (s, 1 H), 4.02 (d, *J* = 10.0 Hz, 1 H), 3.85 (s, 3 H), 3.78 (s, 1 H), 3.60 (d, *J* = 10.8 Hz, 1 H), 2.13-2.06 (m, 1 H), 0.57 (d, *J* = 6.4 Hz, 3 H) ppm; ^{13}C NMR (100 MHz, $CDCl_3$): δ = 147.29, 144.93, 135.82, 134.13, 131.99, 129.73, 129.24, 123.16, 116.89, 116.66, 114.58, 114.36, 114.13, 111.32, 63.97, 56.45, 52.70, 41.78, 16.82 ppm; MS: *m/z* = 398.2 (M+1). Anal. Calcd for $C_{23}H_{21}ClFNO_2$: C, 69.43, H, 5.32, N, 3.52. Found: C, 69.60, H, 5.51, N, 3.73.

4-(6-chloro-2-(4-chlorophenyl)-3-methyl-1,2,3,4-tetrahydroquinolin-4-yl)-2-methoxy phenol (4e)

White amorphous solid; m. p. 192-193 °C; ^{1}H NMR (400 MHz, $CDCl_3$): δ = 7.42-7.37 (m, 2 H), 7.36-7.33 (m, 2 H), 6.97-94 (m, 1 H), 6.88 (d, *J* = 8.0 Hz, 1 H), 6.72 (dd, *J* = 1.6, 8.0 Hz, 1 H), 6.63-6.59 (m, 2 H), 6.52-6.48 (m, 1 H), 5.56 (s, 1 H), 4.08 (d, *J* = 10.4 Hz, 1 H), 3.88 (s, 1 H), 3.85 (s, 3 H), 3.64 (d, *J* = 11.2 Hz, 1 H), 2.20-2.05 (m, 1 H), 0.56 (d, *J* = 6.4 Hz, 3 H) ppm; ^{13}C NMR (100 MHz, $CDCl_3$): δ = 147.32, 144.99, 135.44, 134.42, 130.18, 129.80, 129.34, 127.46, 123.12, 114.67, 111.35, 63.86, 56.48, 52.39, 41.49, 32.03, 23.10, 16.79, 14.57 ppm; MS: *m/z* = 414.4 (M+1). Anal. Calcd for $C_{23}H_{21}Cl_2NO_2$: C, 66.67, H, 5.11, N, 3.38. Found: C, 66.98, H, 5.43, N, 3.60.

4-(8-chloro-2-(4-chlorophenyl)-3-methyl-1,2,3,4-tetrahydroquinolin-4-yl)-2-methoxy phenol (4f)

White amorphous solid; m. p. 185-186 °C; ^{1}H NMR (400 MHz, $CDCl_3$): δ = 7.41-7.35 (m, 4 H), 7.09 (dd, *J* = 2.0, 7.6 Hz, 1 H), 6.87 (d, *J* = 8.0 Hz, 1 H), 6.72 (dd, *J* = 2.0, 8.0 Hz, 1 H), 6.60 (d, *J* = 2.0 Hz, 1 H), 6.51-6.45 (m, 2 H), 5.52 (s, 1 H), 4.60 (s, 1 H), 4.14 (d, *J* = 10.0 Hz, 1 H), 3.83 (s, 3 H), 3.70 (d, *J* = 11.2 Hz, 1 H), 2.17-2.04 (m, 1 H), 0.57 (d, *J* = 6.8 Hz, 3 H) ppm; ^{13}C NMR (100 MHz, $CDCl_3$): δ = 146.83, 144.44, 140.79, 135.47, 133.79, 129.21, 128.88, 128.69, 128.46, 127.01, 122.78, 117.79, 117.21, 114.12, 110.93, 63.09, 56.02, 52.20, 41.16, 16.36 ppm; MS: *m/z* = 414.2 (M+1). Anal. Calcd for $C_{23}H_{21}Cl_2NO_2$: C, 66.67, H, 5.11, N, 3.38. Found: C, 66.98, H, 5.38, N, 3.62.

4-(2-(4-chlorophenyl)-8-fluoro-3-methyl-1,2,3,4-tetrahydroquinolin-4-yl)-2-methoxy phenol (4g)

White amorphous solid; m. p. 180-182 °C; ^{1}H NMR (300 MHz, $CDCl_3$): δ = 7.40-7.33 (m, 4 H), 6.88-6.78 (m, 2 H), 6.72 (dd, *J* = 1.8, 8.1 Hz, 1 H), 6.61 (d, *J* = 2.1 Hz, 1 H), 6.50-6.43 (m, 1 H), 6.37 (d, *J* = 7.8 Hz, 1 H), 5.55 (s, 1 H), 4.23 (s, 1 H), 4.10 (d, 9.9 Hz, 1 H), 3.83 (s, 3 H), 3.71 (d, *J* = 10.8 Hz, 1 H), 2.17-2.08 (m, 1 H), 0.58 (d, *J* = 6.6 Hz, 3 H) ppm; ^{13}C NMR (100 MHz, $CDCl_3$): δ = 151.55, 149.18, 146.77, 144.41, 140.78, 135.63, 133.73, 133.45, 129.23, 128.81, 125.13, 125.10, 122.72, 116.46, 116.39, 114.08, 112.41, 110.99, 62.74, 56.01, 51.97, 41.40, 16.37 ppm; MS: *m/z* = 398 (M+1). Anal. Calcd for $C_{23}H_{21}ClFNO_2$: C, 69.43, H, 5.32, N, 3.52. Found: C, 69.71, H, 5.53, N, 3.78.

4-(6-bromo-2-(4-chlorophenyl)-3-methyl-1,2,3,4-tetrahydroquinolin-4-yl)-2-methoxy phenol (4h)

White amorphous solid; m. p. 187-188 °C; ^{1}H NMR (400 MHz, $CDCl_3$): δ = 7.38-7.32 (m, 4 H), 7.07-7.04 (m, 1 H), 6.88 (d, *J* = 8.0 Hz, 1 H), 6.71-6.67 (m, 2 H), 6.60 (d, *J* = 2.0 Hz, 1 H), 6.40 (d, *J* = 8.4 Hz, 1 H), 5.54 (s, 1 H), 4.07 (d, *J* = 9.6 Hz, 1 H), 4.02 (s, 1 H), 3.85 (s, 3 H), 3.64 (d, *J* = 10.8 Hz, 1 H), 2.11-2.04 (m, 1 H), 0.55 (d, *J* = 6.4 Hz, 3 H)

ppm; ^{13}C NMR (100 MHz, $CDCl_3$): δ = 146.85, 144.52, 143.74, 140.86, 135.07, 133.75, 132.45, 129.80, 129.15, 128.81, 127.69, 122.68, 115.24, 114.29, 110.98, 109.41, 63.22, 56.03, 51.94, 41.25, 16.32 ppm; MS: *m/z* = 458 (M+1); Anal. Calcd for $C_{23}H_{21}BrClNO_2$: C, 60.21, H, 4.61, N, 3.05. Found: C, 60.43, H, 4.86, N, 3.29.

4-(2-(4-chlorophenyl)-3,6-dimethyl-1,2,3,4-tetrahydroquinolin-4-yl)-2-methoxy phenol (4i)

White amorphous solid; m. p. 186-187 °C; ^{1}H NMR (400 MHz, $CDCl_3$): δ = 7.38-7.32 (m, 4 H), 6.87 (d, *J* = 8.0 Hz, 1 H), 6.80 (d, *J* = 8.0 Hz, 1 H), 6.73 (dd, *J* = 1.6, 8.0 Hz, 1 H), 6.64 (d, *J* = 1.6 Hz, 1 H), 6.46 (d, *J* = 8.0 Hz, 1 H), 6.41 (s, 1 H), 5.52 (s, 1 H), 4.06 (d, *J* = 10.0 Hz, 1 H), 3.89 (s, 1 H), 3.84 (s, 3 H), 3.66 (d, *J* = 10.8 Hz, 1 H), 2.14-2.08 (m, 4 H), 0.55 (d, *J* = 6.4 Hz, 3 H) ppm; ^{13}C NMR (100 MHz, $CDCl_3$): δ = 146.71, 144.21, 142.49, 141.44, 136.32, 133.45, 130.43, 129.23, 128.68, 127.61, 127.06, 125.62, 122.81, 113.99, 113.81, 111.13, 63.53, 56.04, 52.27, 41.96, 20.52, 16.44 ppm; MS: *m/z* = 394.6 (M+1). Anal. Calcd for $C_{24}H_{24}ClNO_2$: C, 73.18, H, 6.14, N, 3.56. Found: C, 73.40, H, 6.36, N, 3.79.

ADME-Toxicity prediction

The molecular descriptors of synthesized compounds **4a-i** are optimized using QSAR properties. The SAR activity of these compounds is significantly helps to understand pharmacokinetics to derive physicochemical properties and predict biological activity such as absorption, distribution, metabolism, excretion and toxicity (ADMET). The AdmetSAR [36] helps to evaluate biologically active molecules and eliminate the biologically poor active lead molecules which contain undesirable functional groups based on Lipinski rule. The statistical calculation for lead molecules includes surface area, geometry and fingerprint properties which help to understand biologically important end points. Aqueous solubility (PlogS), Blood-Brain Barrier Penetration (QPlogBB), intestinal absorption (logHIA) [37], Hepatotoxicity, Caco-2 cell permeability (QPPCaco) also helps to understand drug metabolism for top docking lead molecules [38]. Further, to predict the toxicity of lead molecules with intraperitoneal, oral, intravenous and subcutaneous toxic effects of blood, cardiovascular system, gastrointestinal, kidney, liver and lungs to calculate sensitivity, specificity and area under the curves (AUC) that will predicts the linearity of compounds.

Selection of target protein

The disease target 3D crystal protein structures are directly downloaded from the Protein data bank (PDB). The inflammatory protein (PDBID: 4EJ4), cancer protein (PDB ID: 1S63), retinoic acid receptor (PDB ID: 1DSZ), microbial response protein (PDBID: 1C4K), parasitic response receptor (PDB ID: 4AIB) and cholesterol esterase protein (PDBID: 2OBD) is biological inactive proteins helps for disease targets. The conformational protein structure is modeled and visualized using Swiss PDB Viewer. The quality of 3D protein structures of residue-by-residue geometry with stereo chemical parameters is evaluated using PROCHECK, WHATCHECK, ERRAT and Verify3D. The reference compounds such as Indomethacin, Camptothecin, Tretinoin, tetracycline, Lovastatin, and metronidazole are directly downloaded from DrugBank 2.5 database [39] and they are potential competitive inhibitor against target proteins. The pharmacological activity and molecular optimization were calculated using Hyperchem 7.0 Professional [40].

Active site prediction

A prediction of an active site and ligand binding sites of evaluated 3D protein structure by using CastP web server and this helps to calculate topological surface area and surface volume of predicted pockets. These pockets contain electrostatic and van-der-waals forces that locate energetically binding ligands based on ranks of energetical clusters. These probable ligand binding pockets are calculated accordingly with geometric accuracy of RMSD and superimposition of the target to its native structure. RMSD depends on the number of equivalent atom pair of both proteins was compared, which in turn depends upon the maximum allowed distance between atom pairs.

Molecular docking

Molecular docking studies of biologically inactive protein with synthesized lead compounds were carried out by using AutoDock 4.2 and Auto Dock Tools (ADT) v 1.5.4 from the Scripps Research Institute. The AutoDock helps to add hydrogen to polar hydrogens those are bonded to electronegative atoms like nitrogen and oxygen. Detection of Gasteiger charges within active sites of amino acids was computed and the charges are spread across total residue of polar and non-polar hydrogen bonds. Through selecting a flexible and rigid molecule to create grid map of size 80x80x80 from x, y and z-axis for different grid parameters and the resultant compounds were used to compute molecular stimulation parameters like Lamarckian genetic algorithm of population size 150, the mutation rate of 0.02 and crossover rate of 0.8, these simulations were performed up to 2.5 million energy and the evaluations were maximum at 27000 generations. Each simulation was carried about 10 times which ultimately yielded 10 docked conformations. From this, the lowest energy conformations were regarded as the best binding conformations. The results were analyzed based on clusters of RMSD, SAR activity and hydrogen bonding interactions. At the end, the reverse validation processes ensured the identified hits that fitted with generated Pharmacological models and active sites target proteins. Since all the parameters were required for molecular docking, the Pharmacophore mapping were consequently fixed and used in regular process.

RESULTS AND DISCUSSION

Chemistry

Initially, a mixture of p-chloro aniline (1 mmol) and benzaldehyde (1 mmol) in acetic acid was stirred at room temperature (25 °C) for 20 min. To this stirred mixture, the *trans*-isoeugenol was added and the reaction mixture was refluxed for 10 hr, in which the reaction occurred smoothly to generate 4-(6-chloro-3-methyl-2-phenyl-1,2,3,4-tetrahydroquinolin-4-yl)-2-methoxyphenol (**4b**) in 70 % yield. The result of the reactions of different anilines (**1a-i**) and benzaldehydes (**2a-i**) with *trans*-isoeugenol (**3**) to get novel 2-methoxy-4-(3-methyl-2-phenyl-1,2,3,4-tetrahydroquinolin-4-yl) phenol derivatives (**4a-i**) are summarized in scheme 1 and table 1. The yields of the products were found to be in the range of 60-70 %. The progress of the reaction was continuously monitored by TLC (petroleum ether/ethyl acetate, 9:1 v/v) and the products were subsequently identified by LC-MS analysis. The substitution F, Cl, Br, Me, -O-CH_2O- in all new 2-methoxy-4-(3-methyl-2-phenyl-1,2,3,4-tetrahydroquinolin-4-yl)phenol derivatives (**4a-i**) were varied appropriately on phenyl ring at 2nd position of tetrahydroquinoline and phenyl ring fused with piperdinyl ring to find out their ability to dock with selected proteins. Thus this procedure can be applied to generate large variety of isoeugenol coupled tetrahydroquinolines, which resembles the structure of naturally occurring tetrahydroquinolines possesses diverse biological properties [10].

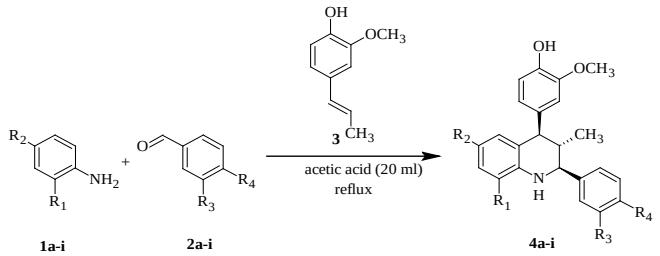

Scheme 1: Synthesis of 2-methoxy-4-(3-methyl-2-phenyl-1,2,3,4-tetrahydroquinolin-4-yl)phenols (4a-i)

Table 1: Reaction of anilines, benzaldehydes and *trans*-isoeugenol in acetic acid at reflux temperature

Entry	Anilines	Products	Time	Yields (%)[a]	m. p.(°C)
4a	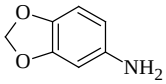	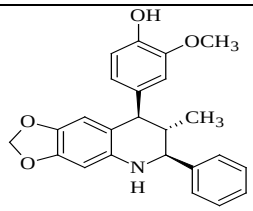	12 hr	65	220-221
4b	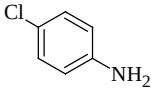	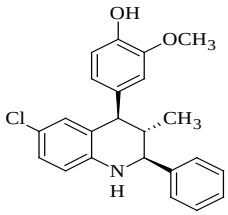	10 hr	70	155-156
4c	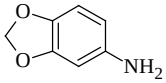	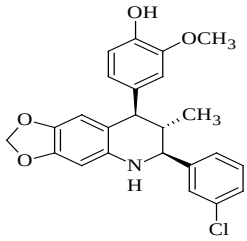	14 hr	70	194-195
4d	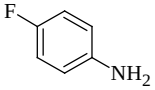	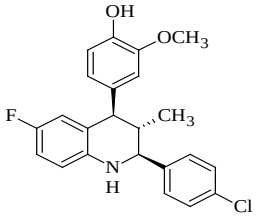	8 hr	60	190-191
4e	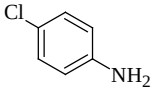	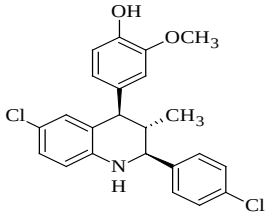	10 hr	65	192-193
4f	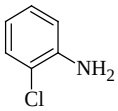	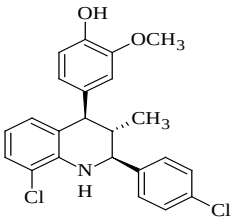	14 hr	60	185-186
4g	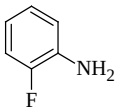	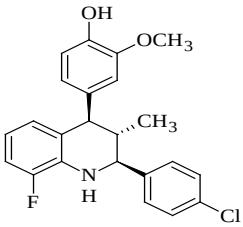	12 hr	65	180-182
4h	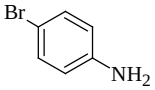	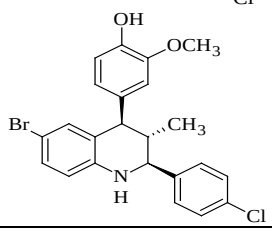	10 hr	65	187-188

4i	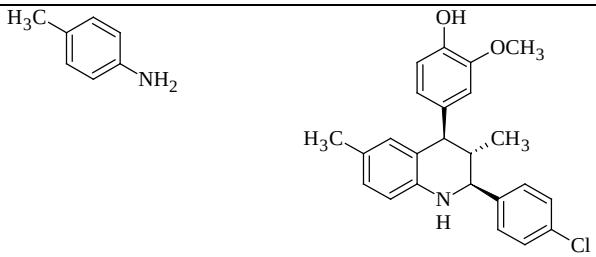	16 hr	70	186-187

The prediction of ^{1}H NMR spectrum of compound 4g exhibited doublet at δ = 0.58 corresponds to C_3-CH_3 protons, multiplet at δ = 2.08-2.17 corresponds to C_3-H proton, doublet at δ = 3.71 corresponds to C_2-H, Singlet at δ = 3.83 corresponds to $C_{3'}$- OCH_3 protons, doublet at δ = 4.10 corresponds to C_4-H, singlet at δ = 4.23 corresponds to -NH, singlet at δ = 5.55 corresponds to -OH. The peaks of 10 aromatic protons have appeared in the expected region of δ = 6.36-7.40 and the number of protons is in accordance with the expected structure.

Additional support to elucidate the structures is obtained from ^{13}C NMR spectrum of these compounds. The appearance of peaks at δ = 16.37, 41.40, 51.97, 56.01, 62.74, 112.23, 112.41, 114.08, 116.39, 116.46, 122.72, 125.10, 125.13, 128.81, 129.23, 133.45, 133,73, 135.63, 140.78, 144.41, 146.77, 149.18, 151.55 corresponds to –CH_3, C_3, C_4, -OCH_3, C_2, $C_{2'}$, C_7, $C_{5'}$, C_6, C_{10}, $C_{6'}$, C_5, C_{13}, C_{15}, C_{12}, C_{16}, C_{14}, C_9, $C_{1'}$, C_{11}, $C_{4'}$, $C_{3'}$, C_8 carbon atoms respectively. The mass spectrum of 4g was recorded as additional evidence to authenticate the structure assign to compound 4g. The compound 4g exhibited M+1 peak at *m/z* = 398. From all these spectral evidences the structure of 4g has been confirmed. Similarly structures of all other derivatives were established and presented in an experimental section.

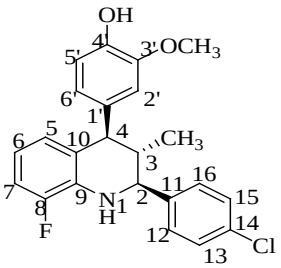

4-(2-(4-chlorophenyl)-8-fluoro-3-methyl-1,2,3,4-tetrahydroquinolin-4-yl)-2-methoxy-phenol(4g)

The stereochemical relationship between C_2, C_3 and C_4 substituents was determined using ^{1}H NMR spectrum. The ^{1}H NMR spectral analysis of compound **4g** shows the appearance of three doublets assignable to the protons of C_2-H (δ = 3.71, *J* = 10.8 Hz), C_4-H (δ = 4.10, *J* = 9.9 Hz), and C_3-CH_3 (δ = 0.58, *J* = 6.6 Hz). These ^{1}H NMR coupling constants indicated that the C_2-H and C_4-H are diaxial to each other (Structure 2, fig. 2).

Thus the aryl groups on C-2 and C-4 are both pseudo-equatorial and hence they are *cis* to each other (Structure 1, fig. 2) [41-43]. Similarly the stereochemical relations of all other compounds were established.

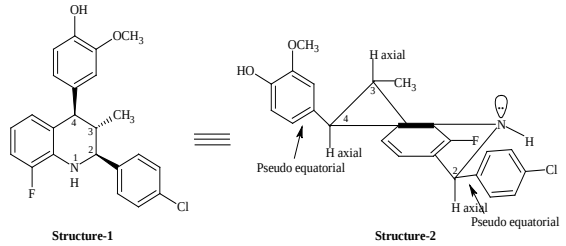

Fig. 2: 4-(2-(4-chlorophenyl)-8-fluoro-3-methyl-1,2,3,4-tetrahydroquinolin-4-yl)-2-methoxy-phenol(4g)

***In silico* pharmacophore analysis of target protein based on lead molecule activity**

The microbial, cancer, retinoic acid receptor, inflammatory, cholesterol ester transferases and parasitic protein receptor structures were directly used for molecular docking. The 3D x-ray crystal structure of analgesic and inflammatory proteins such as 4EJ4 has 3.40 Å resolutions contain signaling protein of opioid receptor has been a excellent target for analgesic and inflammatory disease [44]. Another protein such as Human protein farnesyltransferase complexes with L-778,123 and FPP acts as anticancer, the crystal structures of this protein is 1S63 with 1.90Å. The protein FTase inhibitors of cancer are significant target for development anticancer and antimalarial therapeutics.

Another protein such as assays of retinoid-like receptors (PDB ID: 1C4K, 1DSZ) activates the retinoic acid receptor on ornithine decarboxylase enzyme helps in lactobacillus bacterial growth and disease progression. The correlation between retinoic acid and ornithine decarboxylase shows decrease in cell proliferation and helps for antimicrobial activity within retinal cells [45, 46]. Structural insight of tetrahydroquinolines resistant ornithine decarboxylase from Entamoeba histolytica shows antiinfectious diseases (PDBID: 4AIB) [47].

Another protein such as Cholesteryl ester transfer protein (CETP) (PDBID: 2OBD) [48] shuttles various lipids between lipoproteins, resulting in the net transfer of Cholesteryl esters from atheroprotective, high-density lipoproteins (HDL) to atherogenic, lower-density species. Inhibition of CETP raises HDL cholesterol and may potentially be used to treat cardiovascular disease [49].

The selected protein structures are validated using SAVS. Thus, stereo-chemical activity and quality were presented in table 2. The resultant overall modeled structures are potentially used for rigid docking against 2-methoxy-4-(3-methyl-2-phenyl-1,2,3,4-tetra hydroquinolin-4-yl)phenol (**4a-i**) [50].

Table 2: Geometry optimization of 3D modeled protein using the Swiss PDB viewer and the resultant quality was predicted using SAVS

Proteins	Procheck	Overall Quality factor	RMSD	Q-score	Average Z-score	SDM	Ramachandran Plot
1S63	100%	100	0.1	0.702	-0.664	0.85	96.3%
1C4K	91.36%	86.533	0.7	0.654	-1.202	0.07	87.9%
1DSZ	95.63%	100%	1.6	0.694	-0.782	2.77	90.3%
4AIB	96.47	83.851	1.9	0.626	-1.683	0.67	88.9%
4EJ4	62.98	96.172	0.9	0.567	-2.372	-3.96	91.6%
2OBD	86.26	96.983	0.3	0.599	-1.993	-0.83	90.9%

The Quality assessment of modeled proteins Q-score ranges from zero to one where 1 represented the identical structures and 0 represented the dissimilar structure, Z-score is to identify the protein fold from native structure and ranges from 0 to 1 (0-native protein model, 1 is poor structure that is not used for model). SDM is ranges from 0 to 1 (0 is highly significant with the native structure, 1 is less significant has less model) RMSD shows the significant difference of target and template modeling.

The biological property of all modeled protein structures are used to predict ligand binding and active site amino acids using CastP. The amino acids involved in dimerization with different disease shows strong structural insight into its mechanism of drug interaction. The active site amino acids and the surface area were listed in table 3. The surface energy of active site amino acids that shows minimized free energy was calculated from electrostatic and Vander-Waals interactions between residues of complex proteins.

Table 3: Active site and ligand binding site prediction using Q-site Finder

Protein ID	Active site amino acids	Surface Area	Surface volume
1S63	Gln233, Asn234, Trp235, TYR241, Asn269, Ser272, Gln285, Asp286, Ala330, Gly337,	635.5	810.3
1C4K	Ser198, Ser199, Asn202, Sis223, Gln288, Gly295, Asn316, Ala318, Ser352, His354, Lys355	721.4	1990.3
1DSZ	Cys1171, Cys1177, Cys1187, Cys1190	579.3	941.4
4AIB	Arg51, Cys53, Lys74, Glu94, Asp95, Ile96, Thr97, His118, Met140, Tyr218, Leu219, Ile255	1049.4	715.7
4EJ4	Asp128, Tyr129, Met132, Lys214, Val217, Trp274, Ile277, Val281, Trp284, Leu300, Ile304, Tyr308	1526.3	3133.6
2OBD	Asn296, Leu397, Thr398, Glu399, Ser401, Ser402, Glu403,	3303	5519

Pharmaco Kinetics properties

In silico screening ADMET (Absorption, Distribution, Metabolism, Excretion and Toxicity) profiles

There are many compounds with poor bioavailability shows less effective against disease. To solve this problem, predicting bioavailability properties will be great advantage for drug development. Hence using computer based methods like ADMET and SAR tools the molecular descriptors and drug likeliness properties was studied.

The pharmacokinetic properties are represented in table 5. The coefficient of blood/brain barrier penetration (logB/B) was computed and access with central nervous system (CNS). The CNS activity was computed on -2 (inactive) to +2 (active) scales which show all the molecules are displayed within acceptable range.

The interpretation of test compounds with references shows that the compounds 4b, 4d, 4e, 4f, 4g, 4h and 4i were in good acceptable range and hence, they can be used to make an oral absorption and transport proteins and metabolizing enzymes and maintain homeostatic condition of CNS by separating blood/brain barrier. The intestinal absorption (log_{HIA}) and Caco-2 cell permeability (PCaco-2) within the range of -2 poor absorption and +2 more absorption the compounds are more permeable in intestine and helps for good transport of drug metabolic compounds. It was noticed that the reference molecules enhance the bioavailability properties that leads to less toxic effects against the target protein. The functional groups of compounds such as Br, Cl, F, Me, -O-CH_2-O- had more logP values with partial co-efficient of drug has greatest retention with in human intestine and also has string involvement in drug metabolism.

The logPGI (substrate) and non-inhibitors has drug-drug interaction within tissue that transforms xenobiotics of vigorous reduction of drug absorption and released more bile (liver) and urine (kidney) [45].

The reference range of -5 (poor) to +1 (good) and substrate inhibitor from 0 to 1 in which the reference and test compounds (**4a-i**) shows good activity with human intestinal absorption and metabolism. The aqueous solubility of compounds lies with range of 0 (poor) to 2 (good), showed that all the molecules had good solubility and $logP_{app}$ stated that butein and butin had good permeability on lipid absorption and metabolism. While the reference compounds were came within acceptable range and all test compounds also have acceptable range (Table 4).

From the overall results it was predicted that test compounds have good drug like, lead like and fragment like properties which are strongly accepts for pharmacokinetic and toxicity properties (fig. 2a-g).

Table 4: ADME and pharmacological parameters prediction for the ligands 4a-i using admet SAR toolbox

Ligand	PlogBB[a]	log_{HIA}[c]	PCaco[b]	logpGI (substrate)[d]	logpGI (non-Inhibitor)[e]	PlogS[f]	logpapp[g]
4a	0.5847	0.9514	0.5955	0.6024	0.8148	-3.6508	1.0260
4b	0.8939	0.9941	0.7395	0.5160	0.8299	-4.5040	1.5530
4c	0.5486	0.9585	0.5754	0.6146	0.8822	-4.3697	1.0631
4d	0.9173	0.9972	0.7179	0.5156	0.7688	-4.3746	1.5189
4e	0.8939	0.9941	0.7395	0.5160	0.8299	-4.5040	1.5530
4f	0.8939	0.9941	0.7395	0.5160	0.8299	-4.5040	1.5530
4g	0.9173	0.9972	0.7179	0.5156	0.7688	-4.3746	1.5189
4h	0.8880	0.9959	0.7076	0.5751	0.7950	-4.6033	1.5185
4i	0.8948	0.9935	0.7387	0.5225	0.7513	-4.5805	1.6586
Indomethacin	0.9381	0.9509	0.5857	0.6360	0.9313	-4.6825	0.6287
camptothecin	0.6345	0.8410	0.5555	0.6039	0.7852	-3.0369	1.1839
Tetracycline	0.9841	0.8006	0.7439	0.7910	0.8025	-3.0575	0.7655
Tretinoin	0.9311	0.9925	0.7603	0.6144	0.8912	-3.0895	1.7734
Levostatin	0.9287	0.9452	0.5484	0.7861	0.7046	-5.9475	0.8127
Metronidazole	0.9297	0.9805	0.5365	0.5141	0.8954	-1.3229	0.8033

[a]Predicted blood/brain barrier partition coefficient (1-high penetration, 2- medium penetration and 3- Low penetration). [b]Predicted Caco-2 cell permeability in nm/s (acceptable range: -1 is poor, 1is great). [c]Predicted Human intestinal absorption in nm/s (acceptable range: 0 poor, >1 great). [d]Predicted P-glycoprotein substrate in nm/s (acceptable range of -5 is poor, 1 is great). [e]Predicted P-glycoprotein inhibitor in nm/s (accepted range: 0 to 1), [f]Predicted aqueous solubility, (Concern value is 0-2 highly soluble). [g]Predicted probability of Caco-2 cell permeability in cm/s (Concern value is -1 to 1).

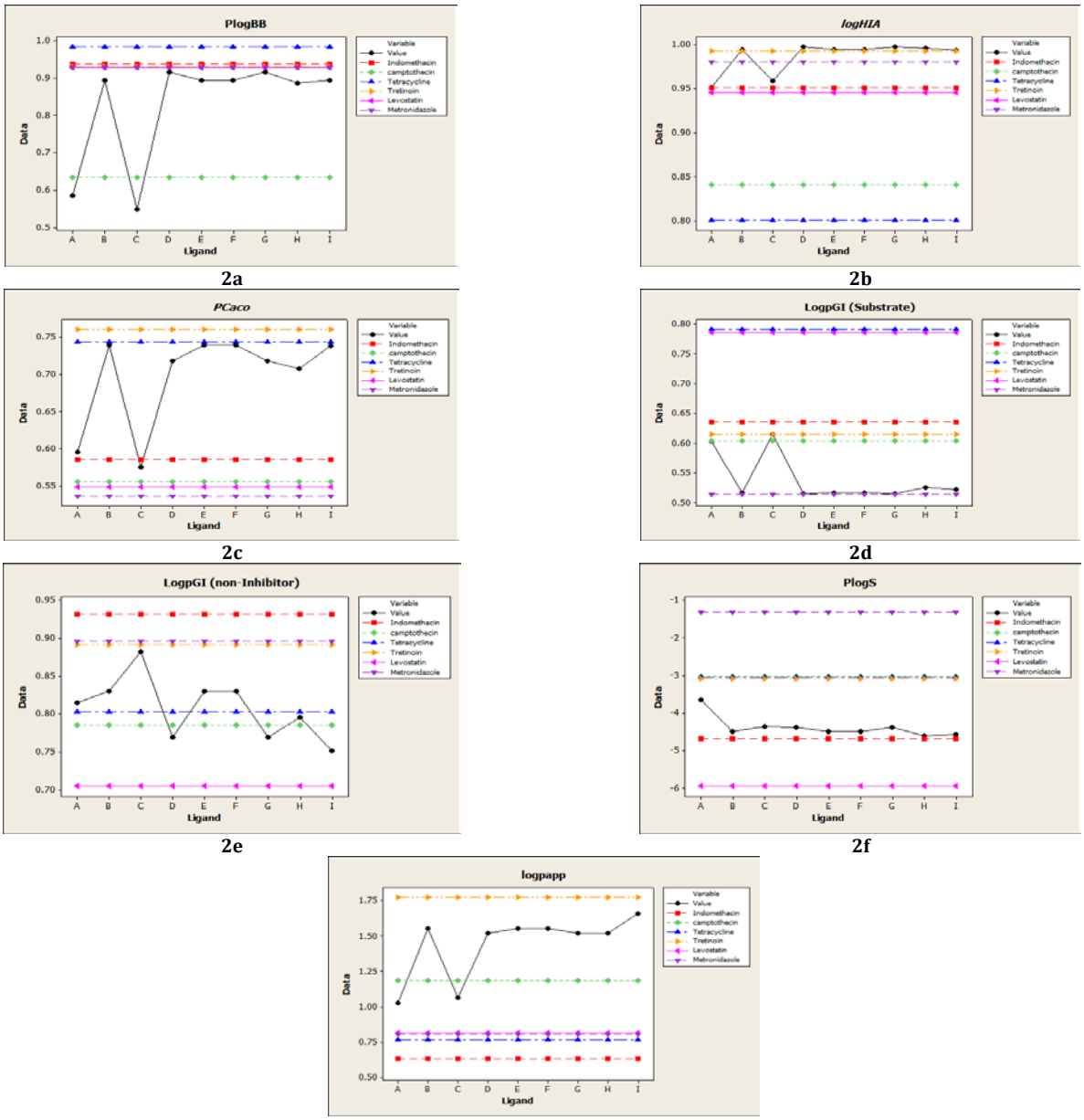

Fig. 2a-g: ADME and Pharmacological parameters of 2-methoxy-4-(3-methyl-2-phenyl-1,2,3,4-tetrahydroquinolin-4-yl)phenols (4a-i) using isoeugenol through admet SAR tool box against reference drugs

Table 5: LD_{50} and probability of health effects of 2-methoxy-4-(3-methyl-2-phenyl-1,2,3,4-tetrahydroquinolin-4-yl)phenols (4a-i) using ACD/ I-Lab 2.0

ADME-TOX Parameters	4a	4b	4c	4d	4e	4f	4g	4h	4i
Intraperitoneal[a]	340 (0.40)	280 (0.18)	380 (0.46)	350 (0.16)	260 (0.14)	230 (0.1)	140 (0.24)	230 (0.15)	160 (0.26)
Oral[a]	390 (0.27)	630 (0.23)	390 (0.28)	520 (0.23)	430 (0.18)	420 (0.25)	340 (0.15)	690 (0.28)	460 (0.19)
Intravenous[a]	45 (0.37)	25 (0.22)	47 (0.39)	26 (0.25)	26 (0.2)	23 (0.39)	16 (0.23)	33 (0.14)	18 (0.02)
Subcutaneous[a]	120 (0.22)	130 (0.26)	86 (0.15)	120 (0.37)	100 (0.34)	61 (0.15)	110 (0.18)	140 (0.15)	82 (0.16)
Blood effect[b]	0.87	0.33	0.94	0.44	0.43	0.34	0.35	0.25	0.59
Cardiovascular system effect[b]	0.68	0.71	0.69	0.76	0.73	0.73	0.76	0.73	0.67
Gastrointestinal system effect[b]	1	0.65	1	0.98	0.98	0.98	0.98	0.98	0.98
Kidney effect[b]	0.71	0.49	0.78	0.74	0.54	0.54	0.7	0.59	0.59
Liver effect[b]	0.95	0.45	0.96	0.49	0.49	0.49	0.49	0.47	0.47
Lung effect[b]	0.91	0.44	0.91	0.93	0.92	0.92	0.93	0.92	0.91

[a]Estimated LD_{50}-mouse value in mg/kg after intraperitoneal, oral, intravenous and subcutaneous administration, [b]Estimated probability of blood, gastrointestinal system, kidney, liver and lung effect at therapeutic dose range of compounds **4a-i**. The drugs with moderate effect on reliability index (>0.5). The drugs with border line effect on reliability index (>0.3, <0.5).

The toxicity of the 2-methoxy-4-(3-methyl-2-phenyl-1,2,3,4-tetrahydroquinolin-4-yl)Phenols (**4a-i**) were predicted based on lethal dosages and functional ranges in different tissues. The LD_{50} mouse and probability of health effects were predicted using ACD/ I-Lab 2.0 (guest).

The toxicity of selected compounds was listed in table 5. The LD_{50} of potential compounds detects the cumulative potential of acute toxicity that administered through oral, intraperitonial, intravenous and subcutaneous on mouse models. The comparative analysis of reference compounds with test compounds on oral, subcutaneous, intraperitonial and intravenous is lowers when compared to reference molecules.

The toxicity results suggests that the compounds **4a-i** have less toxic effect in internal tissues and no side effect was observed in the tested dosages (Table 5).

Further the toxicity was tested with different organs to check adverse effects of organs and their systems (blood, cardiovascular system, gastrointestinal system, kidneys, liver, and lungs) within the therapeutic dose range. The probability of health effects revealed that the 2-methoxy-4-(3-methyl-2-phenyl-1,2,3,4-tetra hydro quinolin-4-yl)Phenols (**4a-i**) had very less toxic effect on blood, cardiovascular, gastrointestinal, kidney, liver and lung respectively.

Molecular docking studies of synthesized 2-methoxy-4-(3-methyl-2-phenyl-1,2,3,4-tetrahydroquinolin-4-yl)phenols (4a-i)

The docking simulation technique was considered as direct study on 3D structures of known functional characteristic proteins, which is a detailed study of intermolecular interaction with the ligands. The different functional characteristic of inflammatory, malarial, microbial, parasitic, tumor and retinoic acid receptor (RARβ) proteins was performed to predict active sites of 4EJ4, 1S63, 1DSZ, 2ON3, 1C4K, 4AIB and 2OBD through Auto dock program. The experimental values were observed based on hydrogen bonds, inhibitory constant and docking scores of compounds **4a-i** as predicted in table 6.

Molecular docking of compounds 4a-i with inflammatory protein using reference drug Indomethacin

The reference molecule such as Indomethacin was strongly interacting with inflammatory protein. The 3D protein structure with reference drug has 3 hydrogen bonds with active site amino acids Gln203 and Tyr262. The protein structure shows strong interactions with test drugs **4c** and **4f** with active site amino acids Arg 210, His107, Ala197, Thr198 and Arg195 of binding energy -16.0728 kcal/mol and -56.5169 kcal/mol respectively (fig. 3a). The less toxicity and LD50 of pharmacokinetics of anti-inflammatory property suggest the synthesized ligands **4a-i** could be a potential drug for the treatment of inflammatory diseases (Table 6a).

Table 6a: Molecular docking results of Indomethacin and compounds 4a-i with inflammatory protein

Ligands	H Bonds	Docking Score	IC50	Amino acids
4a	3	-16.7112	85.98	Ser266, Lys210
4b	3	-14.8443	51.98	His107, Arg170
4c	4	-16.0728	83.11	Arg210, His107
4d	3	-33.352	51.14	Tyr183, Tyr184, Arg170
4e	3	-23.5806	50.24	Ser209, Tyr166
4f	4	-56.5169	41.11	Ala197, Thr198, Arg195
4g	2	-30.8435	57.66	Arg195, Arg175
4h	2	-14.3566	58.09	Ser291
4i	3	-43.6456	47.78	Thr198, Arg195
Indomethacin	3	-13.9304	19.181	Gln203, tyr262

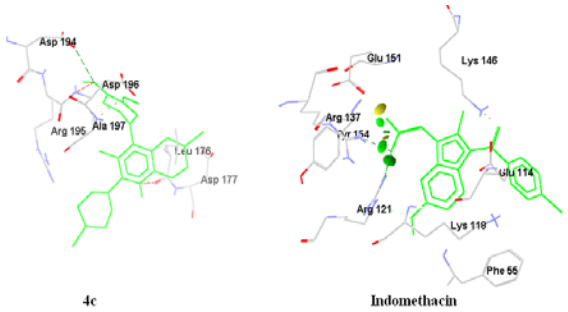

Fig. 3a: Molecular docking images of Indomethacin and compounds 4c with inflammatory protein

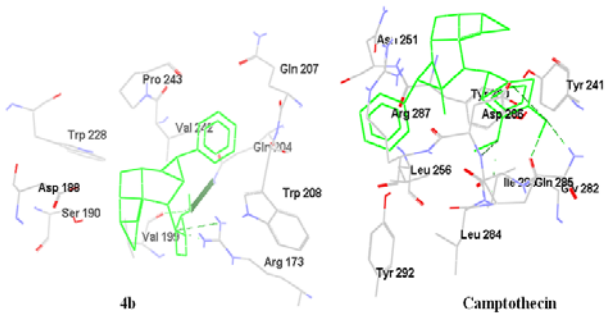

Fig. 3b: Molecular docking images of Camptothecin and compound 4b with cancer protein

Molecular docking of compounds 4a-i with cancer protein using reference drug Camptothecin

The reference drug such as Camptothecin strongly interacts with cancer protein shows 3 hydrogen bonds with interaction energy of -13.5327 kcal/mol within active site amino acids of Glu107 and Arg112. The compounds **4b** and **4f** binds with energy of -8.99845 and -5.70191 kcal/mol (fig. 3b) hence are more effective against tumor causing proteins than remaining derivatives (Table 6b).

Molecular docking of compounds 4a-i with retinoic acid protein using reference drug Tretinoin

The retinoic protein is interacts with existing reference drug Tretinoin form 3 hydrogen bonds within active site amino acids Asn1185 and Arg1186, the interaction energy shows -7.84425 kcal/mol.

The compounds such as 4a have 7 hydrogen bonds with strong interactions within active site amino acids Asn1185 and Arg1309 with interaction energy of -47.423 kcal/mol (fig. 3c). The other compounds such as 4c, 4g and 4h have 4 hydrogen bonds were also shows good binding energy between protein and ligands. Thus, overall results shows that the 2-methoxy-4-(3-methyl-2-phenyl-1,2,3,4-tetrahydroquinolin-4-yl)phenols (4a-i) could be a good target drugs against retinoic disorders (Table 6c).

Molecular docking of compounds 4a-i with microbial protein using reference drug Tetracycline

The microbial protein is interacts with tetracycline drug has 8 hydrogen bonds of energy -19.6519 kcal/mol within active site amino acids Glu532, Pro531, Arg525, Ser534 and Tyr292 (fig. 3d). The ligand 4g shows only 5 hydrogen bonds of energy -

32.9844kcal/mol within active site amino acids Arg155, Gln124, Leu122. The overall results suggest that the reference drug and 4g compound only exhibits strong interaction with microbial protein (Table 6d).

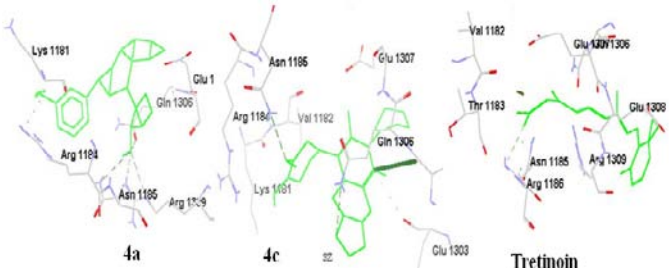

Fig. 3c: Molecular docking images of Tretinoin and compound 4a, 4c with retinoic acid protein

Table 6b: Molecular docking results of Camptothecin and compounds 4a-i with cancer protein

Ligands	H Bonds	Docking Score	IC50	Amino acids
4a	3	-10.7544	114.816	Trp228, Ser190, Arg173
4b	5	-8.99845	73.7759	Asp286, Gln285, Gly282
4c	2	-18.9507	88.8607	Phe55, Lys118
4d	4	-8.21431	106.005	Asp147, Lys146, Glu151
4e	2	-20.0888	113.086	Arg32
4f	5	-5.70191	87.2604	Lys346, Tyr24, Glu33, Thr350, Glu29
4g	4	-6.11935	123.	Arg231, Trp228, Asp188, Ser190
4h	2	-13.3528	80.0437	Lys146, Arg121
4i	2	-5.25854	141.274	Asp188,Arg173
Camptothecin	4	-13.5327	82.5153	Glu107, Arg112

Table 6c: Molecular docking results of Tretinoin and compounds 4a-i with retinoic acid protein

Ligands	H Bonds	Docking Score	IC50	Amino acids
4a	7	-47.423	7989.09	Asn1185, Arg1309
4b	2	-14.7875	4997.88	Gln1164, Tyr1147
4c	4	-29.1262	8018.13	Glu1253, Ser1243
4d	2	-45.9827	4942.04	Asn1185
4e	3	-25.4405	4984.89	Ser1242, Arg1241
4f	3	-22.5136	4991.51	Ser1243, Glu1253
4g	4	-32.2036	4996.67	Lys1194, Ile1179
4h	4	-17.4822	4996.1	Ser1162, Tyr1169
4i	2	-67.9766	5015.48	Arg1264, Gln1306
Tretinoin	3	-7.84429	-89.150	Asn1185, Arg1186

Table 6d: Molecular docking results of Tetracycline and compounds 4a-i with microbial protein

Ligands	H Bonds	Docking Score	IC50	Amino acids
4a	2	-17.4333	8025.21	Tyr240, Arg618
4b	3	-24.4834	5001.5	Trp319, Gln288
4c	2	-18.517	7997.09	Tyr292
4d	3	-16.5024	4982.45	Lys270, Gln624
4e	3	-29.5001	4996.25	Trp319, Lys355
4f	3	-40.9468	5010.31	Thr518, Ser534
4g	5	-32.9844	4945.83	Arg155, Gln124, Leu122
4h	1	-25.4518	5009.09	Arg418
4i	2	-18.9203	5001.21	Gln131, Arg155
Tetracycline	8	-19.6519	140.114	Glu532, Pro531, Arg525, Ser534, Tyr292,

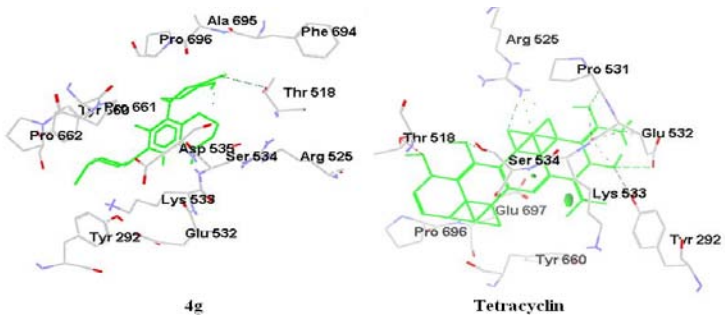

Fig. 3d: Molecular docking images of Tretinoin and compounds 4g with microbial protein

Table 6e: Molecular docking results of Lovastatin and compounds 4a-i with cholesterol esterase protein

Ligands	H Bonds	Docking Score	IC50	Amino acids
4a	2	-7.26397	108.778	Cys325, Met284
4b	2	-7.96008	121.093	Val323, Ser342
4c	3	-8.29829	20.1631	Ser342, Cys325
4d	3	-10.1056	121.364	Cys325
4e	1	-7.53544	85.8409	Ile205
4f	2	-7.63279	84.1989	Ser342, Thr369
4g	2	-7.08915	85.8348	Thr369, Ser342
4h	2	-9.28919	79.4015	Arg282, Asp208S
4i	3	-9.07913	-110.09	Val232, Ser342,
Lovastatin	1	-20.9465	111.037	Arg282

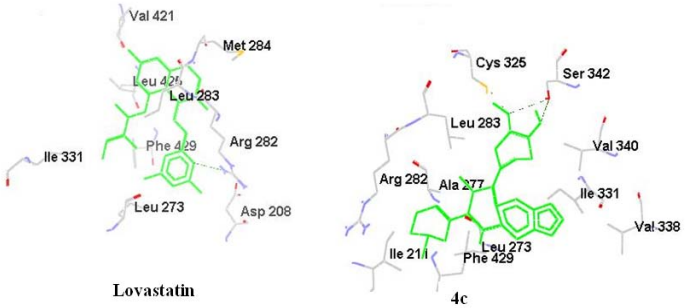

Fig. 3e: Molecular docking images of Lovastatin and compounds 4c with cholesterol esterase protein

Molecular docking of compounds 4a-i with cholesterol ester transferases using reference drug Lovastatin

The Lovastatin shows weekly interaction with cholesterol esterase protein with 1 hydrogen bond. However, the compounds **4c**, **4d** and **4i** show 3 hydrogen bonds within active site amino acids of energy -8.29829 kcal/mol (fig. 3e).

Hence the result shows that the test compounds are moderately active against cholesterol esterase protein receptor (Table 6e).

Molecular docking of compounds 4a-i with parasitic protein using reference drug Metronidazole

The Antiparasitic protein is strongly interacts with Metronidazole compound with active site amino acids of 5 hydrogen bonds of energy -11.4869 kcal/mol (fig. 3f). The all compounds 4a-i shows strong interaction with parasitic protein. The overall results show that the 2-methoxy-4-(3-methyl-2-phenyl-1,2,3,4-tetrahydro quinolin-4-yl)Phenols (4a-i) are found to be the good activators of antiparasitic properties (Table 6f).

Table 6f: Molecular Docking results of Metronidazole and compounds 4a-i with parasitic protein

Ligands	H Bonds	Docking Score	IC50	Amino acids
4a	6	-20.7946	101.494	Phe226, Gly259, Arg260
4b	4	-12.1015	92.9308	Arg142, Gln100, Thr101
4c	7	-1.75917	125.134	Ser188, Phe266, Tyr261, Gly259, Arg260
4d	4	-9.17663	84.5873	Glu257, Glu259, Arg260, Ser188
4e	5	-3.89349	113.675	Tyr363, Lys157, His185, Arg142
4f	3	-9.83094	78.4661	Ser5, Asn359
4g	3	-8.00873	68.3715	Gly225, Phe226
4h	4	-16.2947	109.784	Asp76, Ser99, Tyr363
4i	3	-12.1383	88.9163	Arg142, Lys157, Tyr363
Metronidazole	5	-11.4869	134.649	Arg260, Gln228, Ser188, Gly259, Tyr363

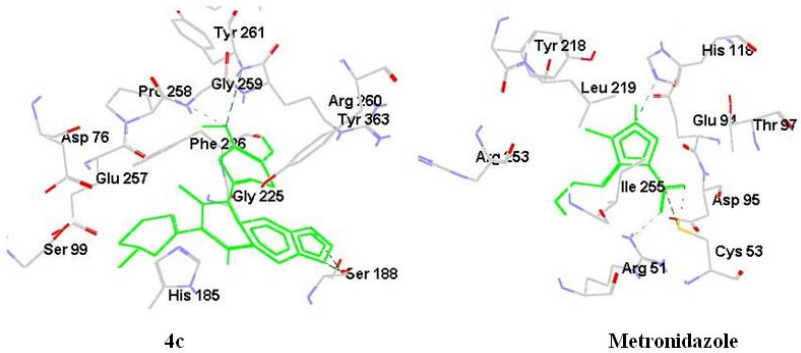

Fig. 3f: Molecular docking images of Metronidazole and compounds 4c with parasitic protein

CONCLUSION

A straight forward, multi component, high yielding, eco friendly, one pot synthesis of novel 2-methoxy-4-(3-methyl-2-phenyl-1,2,3,4-tetrahydroquinolin-4-yl)phenols was described *via* imino Diels-Alder reaction between anilines, benzaldehydes and *trans*-isoeugenol using acetic acid as catalyst and solvent. This procedure was very simple in which one can couple *trans*-isoeugenol into tetrahydroquinoline moiety which resembles the structures of many naturally occurring bioactive tetrahydroquinolines.

The toxicity results suggests that the compounds 4a-i have less toxic effect in internal tissues and no side effect was observed in the test dosages. The docking analysis shows that the compounds 4c and 4f were strongly interacts with active site amino acids Arg210, His107, Ala197, Thr198 and Arg195 of binding energy -16.0728 kcal/mol and -56.5169 kcal/mol with inflammatory protein PDB ID: 4EJ4 for anti-inflammatory properties. The compound 4b and 4f binds with cancer protein PDB ID: 1S63 within active site that shows -8.99845 and -5.70191 kcal/mol of energy and hence these compounds are more effective for antitumor properties. The compound 4a shows 7 hydrogen bonds with retinoic acid protein PDB ID: 1DSZ within active site amino acids Asn1185 and Arg1309 with interaction energy of -47.423 kcal/mol compared to remaining compounds. The compound 4g shows 5 hydrogen bonds with energy -32.9844 kcal/mol within active site amino acids Arg155, Gln124, Leu122 with microbial protein within 1C4K. The compounds 4c, 4d and 4i exhibits 3 hydrogen bonds within active site amino acids of energy -8.29829 kcal/mol, with cholesterol esterase protein PDB ID: 2OBD. Whereas all 4a-i compounds shows strong interaction with parasitic protein PDB ID: 4AIB. In conclusion since all the compounds 4a, 4c, 4f, 4g and 4h were found to exhibits multifunctional activities they can be considered for further clinical trials to prove them as lead molecules to act against microbial, cancer, retinoic acid receptor, inflammatory, cholesterol ester transferases and parasitic diseases.

ACKNOWLEDGMENT

The authors thank Department of Post Graduate Studies and Research in Chemistry, Kuvempu University for providing laboratory facilities and IISc Bangalore for providing spectral data.

CONFLICT OF INTERESTS

Declared None

REFERENCES

1. National Toxicology Program. Toxicology and carcinogenesis studies of isoeugenol (CAS No. 97-54-1) in F344/N rats and B6C3F1 mice (gavage studies). Natl Toxicol Program Tech Rep Ser 2010;551:1-178.
2. Mehmet K. Inhibitory effects of anethole and eugenol on the growth and toxin production of aspergillus parasiticus. Int J Food Microbiol 1990;10:193-9.
3. Long H, Mathieu B, Pascal R, Géraldine M. Chiral phosphoric acid catalyzed inverse-electron-demand aza-diels-alder reaction of isoeugenol derivatives. Org Lett 2012;14:3158-61.
4. Tatsuzaki J, Bastow KF, Nakagawa-Goto K, Nakamura S, Itokawa H, Lee KH. Dehydrozingerone, chalcone, and isoeugenol analogs as *in vitro* anticancer agents. J Nat Prod 2006;69:1445-9.
5. Vladimir VK, Diego RM, Francisco A, Josue SBF, Felipe S, Arturo M. 4-Hydroxy-3-methoxyphenyl substituted 3-methyl-tetrahydroquinoline derivatives obtained through imino Diels-alder reactions as potential antitumoral agents. Lett Drug Des Discovery 2010;8:632-9.
6. Pravin B, Srinivas O, Praveen Kumar S, Vivek B, Kasey R, Laxman N, *et al*. Second generation tetrahydroquinoline-based protein farnesyltransferase inhibitors as antimalarials. J Med Chem 2007;50:4585-605.
7. Richard LB, Min T, Diana FC, Tien TD, Scott MT, Taghreed A, *et al*. Synthesis and biological activity of 1,2,3,4-tetrahydroquinoline and 3,4-(1*H*)-dihydroquinolin-2-one analogs of retinoic acid. Bioorg Med Chem Lett 1997;7:2373-8.
8. Mostafa MG, Fatma AR, Mostafa MH. Design, synthesis and anticancer evaluation of novel tetrahydroquinoline derivatives containing sulfonamide moiety. Eur J Med Chem 2009;44:4211-7.
9. Romina JP, Sabrina L, Adriana BP, Reto B, María RM. Synthesis, stereoelectronic characterization and antiparasitic activity of new 1-benzenesulfonyl-2-methyl-1,2,3,4-tetrahydroquinolines. Bioorg Med Chem 2010;18:142-50.
10. Jiwen L, Yingcai W, Ying S, Derek M, Shichang M, George T, *et al.* Tetrahydroquinoline derivatives as CRTH2 antagonists. Bioorg Med Chem Lett 2009;19:6840-4.
11. Howard CS, Caitlin KC, Jennifer LF, Christine ST, Jessica AS, Enrique LM, *et al*. Synthesis and SAR of cis-1-benzoyl-1,2,3,4-tetrahydroquinoline ligands for control of gene expression in ecdysone responsive systems. Bioorg Med Chem Lett 2003;13:1943-6.
12. Guifang J, Jingwei Z, Jianwei H, Shizheng Z, Jianmin Z. Iodine-promoted imino-Diels–Alder reaction of fluorinated imine with enol ether: synthesis of 2-perfluorophenyl tetrahydroquinoline derivatives. Tetrahedron 2010;66:913-7.
13. Savitha G, Perumal PT. An efficient one pot synthesis of tetrahydroquinone derivatives via Aza Diels-Alder reaction mediated by ceric ammonium nitrate in the oxidation of heteroarylquinolines. Tetrahedron Lett 2006;47:3589-93.
14. Alexander SK, Leon SI, Robert WA. Solid support synthesis of polysubstituted tetrahydroquinolines *via* three-component condensation catalyzed by $Yb(OTf)_3$. Tetrahedron 1998;54:5089-96.
15. Isabelle GD, Philippe G, Rajanbabu TV. Asymmetric synthesis of functionalized 1,2,3,4-tetrahydroquinolines. Org Lett 2001;3:2053-6.
16. Rajagopal N, Paramasivan TP. Imino Diels-alder reactions catalyzed by oxalic acid dihydrate. Synthesis of tetrahydroquinoline derivatives. Synth Commun 2001;31:1733-6.
17. Kimura Y, Kusano M, Koshino H, Uzawa J, Fujioka S, Tani K. Penigequinolones A and B, pollen-growth inhibitors produced by Penicillium sp No 410. Tetrahedron Lett 1996;37:4961-4.
18. Hayashi H, Nakatani T, Inoue Y, Nakayama M, Nozaki H. New dihydroquinolone toxic to *Artemia salina* produced by *Penicillium* sp. NTC-47. Biosci Biotechnol Biochem 1997;61:914-6.
19. Kusano M, Koshino H, Uzawa J, Fujioka S, Kawano T, Kimura Y. Nematicidal alkaloids and related compounds produced by the fungus Penicillium cf. simplicissimum. Biosci Biotechnol Biochem 2000;64:2559-68.
20. He J, Lion U, Sattler I, Gollmick FA, Grabley S, Cai J, *et al*. Diastereomeric quinolinone alkaloids from the marine-derived fungus Penicillium janczewskii. J Nat Prod 2005;68:1397-9.
21. Uchida R, Imasato R, Shiomi K, Tomoda H, Ohmura S. Yaequinolones J1 and J2, novel insecticidal antibiotics from *Penicillium* sp. FKI-2140. Org Lett 2005;7:5701-4.
22. Diego R, Merchan A, Fernando A, Rojas R, Vladimir VK. Highly diastereoselective synthesis of new heterolignan-like 6,7-methylendioxy-tetrahydroquinolines using the clove bud essential oil as raw material. Tetrahedron Lett 2011;52:1388-91.
23. Bindu PJ, Mahadevan KM, Ravikumar Naik TR, Harish BG. Synthesis, DNA binding, docking and photocleavage studies of quinolinyl Chalcones. Med Chem Commun 2014;5:1708-17.
24. Jagadeesh NM, Mahadevan KM, Kumara MN, Prashantha N. Synthesis and molecular docking study of *N*-alkyl/aryl-2-aryl indol-3-yl glyoxylamides as novel anticancer agents. Int J Pharm Pharm Sci 2014;6:921-6.
25. Siddalingamurthy E, Mahadevan KM, Jagadeesh NM, Kumara MN. Synthesis and docking study of 3-(*N*-alkyl/aryl piperidyl) indoles with serotonin-5HT, H1 and CCR2 antihistamine receptors. Int J Pharm Pharm Sci 2014;6:475-82.
26. Jagadeesh NM, Mahadevan KM, Jayadevappa H, Mahesh M, Preenon B. Synthesis and molecular docking studies of 2,3-dialkylindoles and carbazoles with MDM2-p53 and PBR receptor proteins. Am J Pharm Health Res 2014;2:88-102.
27. Siddalingamurthy E, Mahadevan KM, Jagadeesh NM, Kumara MN. Synthesis of indolecarboxamides and their docking studies with H1, 5HT and CCR2 antagonist receptors. Am J Pharm Health Res 2014;2:245-58.
28. Jagadeesh NM, Mahadevan KM, Siddalingmurthy E, Preenon Bagchi. Synthesis and molecular docking studies of 1-trityl-5-azaindazole derivatives. J Chem Pharm Res 2014;6:143-52.

29. Jagadeesh NM, Mahadevan KM, Preenon B. Synthesis, molecular docking and fluorescent properties of novel (*E*)-3-(9-ethyl-9*H*-carbazol-3yl)-1-phenylprop-2-en-1-ones. Int J Pharm Pharm Sci 2014;6:317-25.
30. Siddalingamurthy E, Mahadevan KM, Jagadeesh NM, Kumara MN. Synthesis of novel γ-carboline derivatives and their *in silico* studies on 5HT1, H1 and CCR2 antagonist receptors. Int J Pharm Pharm Sci 2014;6:548-54.
31. Bindu PJ, Mahadevan KM, Ravikumar Naik TR. Sm(III)nitrate-catalyzed one-pot synthesis of furano[3,2c]-1,2,3,4-tetrahydroquinolines and DNA photocleavage studies. J Mol Struct 2012:1020;142-7.
32. Srinivasa A, Mahadevan KM, Vijaykumar H. Imino *Diels-Alder* Reactions: Efficient synthesis of 2-Aryl-4-(2'-oxopyrrolidinyl-1')-1,2,3,4-tetrahydroquinolines catalyzed by antimony (III) sulphate. Monatsh Chem 2008;139:255-9.
33. Bindu PJ, Mahadevan KM, Ravikumar Naik TR. An efficient one-pot synthesis and Photo-induced DNA cleavage studies of 2-chloro-3-(5-aryl-4,5-dihydroisoxazol-3-yl)quinolines. Bioorg Med Chem Lett 2012:22;6095-8.
34. Prabhakara VP, Sherigara BS, Mahadevan KM, Vijaykumar H. Mild and a simple access to diverse 4-amino substituted 2-phenyl-1,2,3,4-tetrahydroquinolines and 2-phenylquinolines based on a multi component imino Diels-Alder reaction. Synth Commun 2010;40:2220-31.
35. Kiran Kumar HC, Mahadevan KM, Prabhakara Varma P, Srinivasa A. One pot Synthesis of medicinally important *cis*-2-Methyl-4-amino substituted-1,2,3,4-tetrahydroquinoline. Chin J Chem 2012;30:534-40.
36. Feixiong C, Weihua L, Yadi Z, Jie S, Zengrui W, Guixia L, *et al*. Admetsar: a comprehensive source and free tool for assessment of chemical ADMET properties. J Chem Inf Model 2012;52:3099-105.
37. Lin JH, Yamazaki M. Role of P-glycoprotein in pharmacokinetics: clinical implications. Clin Pharmacokinet 2003;42:59-98.
38. David L, Olivier S, Hervé G, Maria AM, Bruno OV. FAF-Drugs2:Free ADME/tox filtering tool to assist drug discovery and chemical biology projects. BMC Bioinf 2008;9:396.
39. Wishart DS, Knox C, Guo AC, Shrivastava S, Hassanali M, Stothard P, *et al*. Drug bank: a comprehensive resource for in silico drug discovery and exploration. Nucleic Acids Res 2006;34:668-72.
40. ACD/Chem Sketch Version 12.01 Advanced Chemistry Development, Inc, Toronto; 2009.
41. Arenas DRM, Ruíz FAR, Kouznetsov VV. Highly diastereoselective synthesis of new heterolignan-like 6,7-methylendioxy-tetrahydroquinolines using the clove bud essential oil as raw material. Tetrahedron Lett 2011;52:1388-91.
42. Kouznetsov VV, Bohorquez ARR, Stashenko EE. Three-component imino Diels–Alder reaction with essential oil and seeds of anise: generation of new tetrahydroquinolines. Tetrahedron Lett 2007;48:8855-60.
43. Bohorquez AR, Kouznetsov VV, Doyle MP. Cu (OTf)2-Catalyzed three-component imino diels-alder reaction using propenylbenzenes: synthesis of 2,4-diaryl tetrahydroquinoline derivatives. Lett Org Chem 2011;8:5-11.
44. Reid TS, Long SB, Beese LS. Crystallographic analysis reveals that anticancer clinical candidate L-778,123 inhibits protein farnesyltransferase and geranylgeranyltransferase-I by different binding modes. Biochem 2004;43:9000-8.
45. Vitali J, Carroll D, Choudhury RG, Hackert ML. Three-dimensional structure of the Gly121Tyr dimeric form of ornithine decarboxylase from Lactobacillus 30a. Acta Crystallogr Sect D 1999;55:1978-85.
46. Rastinejad F, Wagner T, Zhao Q, Khorasanizadeh S. Structure of the RXR–RAR DNA-binding complex on the retinoic acid response element DR1. EMBO J 2000;19:1045-54.
47. Preeti P, Tapas S, Kumar P, Tomar S. Structural insight into DFMO resistant ornithine decarboxylase from Entamoeba histolytica: an inkling to adaptive evolution. PloS One 2013;8:533-97.
48. Granier S, Manglik A, Kruse AC, Kobilka TS, Thian FS, Weis WI, *et al*. Structure of the *δ*-opioid receptor bound to naltrindole. Nat 2012;485:400-4.
49. Qiu X, Mistry A, Ammirati MJ, Chrunyk BA, Clark RW, Cong Y, *et al*. Crystal structure of cholesteryl ester transfer protein reveals a long tunnel and four bound lipid molecules. Nat Struct Mol Biol 2007;14:106-13.
50. Freitas MP, Da Cunha EFF, Ramalho TC, Goodarzi M. Multimode methods applied on MIA descriptors in QSAR. Curr Comput Aided Drug Des 2008;4:273-82.